Application of the cluster/site approximation to the calculation of multicomponent alloy phase diagrams

W. Cao [a], Y.A. Chang [a,*], J. Zhu [a], S. Chen [b], W.A. Oates [c]

[a] *Department of Material Science and Engineering, University of Wisconsin, 215 MS&E Building 1509, Madison, WI 53706, USA*
[b] *CompuTherm LLC, 437 South Yellowstone Drive, Madison, Wisconsin 53719, USA*
[c] *Institute for Materials Research, University of Salford, Salford M5 4WT, UK*

Abstract

The cluster/site approximation (CSA) offers computational advantages, without loss of accuracy, over the cluster variation method (CVM) in the calculation of multicomponent phase diagrams. Its ease of use and advantages are illustrated in the calculation of a prototype Cu–Ag–Au fcc order/disorder phase diagram previously calculated using the CVM.
© 2004 Acta Materialia Inc. Published by Elsevier Ltd. All rights reserved.

1. Introduction

Multicomponent alloy phase diagrams are required for technological purposes and their calculation has become an important tool in Materials Science and Engineering. This stems from the fact that it is just not possible, in any reasonable time frame, to obtain the required information by measurements alone.

Solution phase modeling in alloy thermodynamics requires acknowledgement of not only the chemical interactions and excitations but also the elastic interactions which arise from atomic size mismatch. The latter are long ranged and it is necessary to use real and reciprocal space Monte-Carlo (MC) simulations in order to model them satisfactorily [1]. Although software suitable for doing this kind of calculation is available [2], its use for real alloy multicomponent phase diagram calculations (which may involve up to as many as 15 components) is unlikely to replace computationally more efficient although physically less satisfactory approaches.

The simpler approaches which have been used for multicomponent alloys have invariably been constant volume models and they have most often used the point approximation [3]. This is in spite of the fact that this approximation is known to give problems with phase diagram topography, particularly for fcc-based systems, due to the neglect of short range order (SRO) in the configurational calculation. As a result, there has been much interest in using higher order, small cluster, approximations in order to allow for SRO. In this regard, the cluster variation method (CVM) [4–6] has been pre-eminent. In the last three decades, the calculation of both prototype and real alloy phase diagrams, based on the use of the CVM, has been widely used for binary systems. In the case of (constant volume) prototype systems, good agreement is obtained with the results from MC simulations based on the same (short range) energy parameters.

Notwithstanding these successes, a major disadvantage of the CVM has been recognized, i.e., the solution of a large number of nonlinear simultaneous equations

---

* Corresponding author. Tel.: +1 608 262 0389; fax: +1 608 262 8353.

E-mail address: chang@engr.wisc.edu (Y.A. Chang).

is necesssary, particularly when it is used for multicomponent systems. This is because the independent variables in the CVM are essentially the cluster probabilities, of which there are C^n, where C is the number of components and n the number of atoms in the cluster. It is for this reason that the CVM does not seem to have been applied to systems with more than three components and, even for three components, only pair or tetrahedron clusters have been used.

Prior to the introduction of the CVM, Yang and Li [7–10] had suggested a different cluster model (a generalized quasi-chemical model). Whilst this gave more satisfactory results than could be obtained from the point approximation, it did not give the desired topography for the fcc order/disorder phase diagram. Later, Oates and Wenzl [11] noted that the Yang–Li model, which they called the cluster/site approximation (CSA), had the big advantage over the CVM, in so far as the application of small cluster models to multicomponent phases is concerned, that the independent variables are the point probabilities rather than the cluster probabilities. Since there are only $C \times n$ point probabilities as compared with C^n cluster probabilities, the computational advantages of the CSA are obvious. Subsequently, Oates et al. [12] showed how the problems associated with the topography of the fcc order/disorder phase diagram in the CSA could be overcome.

To date, this modified CSA has been used successfully in the calculation of several real alloy binary phase diagrams: Au–Cu [12], Au–Ni [13], Cd–Mg [14], Cr–Ta [15], Al–Ni [16]. As part of our desire to extend these calculations to real multicomponent alloys we report here some results obtained from the application of the CSA to the calculation of some prototype fcc phase diagrams for ternary alloys. The results are compared with those obtained by the CVM.

2. The cluster/site approximation

Unlike the clusters used in the CVM, the clusters in the CSA must be energetically non-interfering, i.e., they are permitted to share only corners but not faces or edges. The result from fulfilling this requirement is that the configurational entropy then involves only the cluster entropy and the single-site entropy, i.e., there are only two terms in the entropy expression. The entropy per site S_m can be written as

$$S_m = \gamma S_n - (n\gamma - 1)S_1, \tag{1}$$

where γ is the number of energetically non-interfering clusters per site. In the nearest neighbor pairwise approximation, as was used by Yang and Li, $\gamma = z/2p$, z being the nearest-neighbor coordination number and p the number of nearest-neighbor pairs in the cluster of size n. The dimensionless cluster and site entropies S_n, S_1 are given

by $S_n = -\sum_i Z_i \ln Z_i$ and $S_1 = -\sum_i X_i \ln X_i$, respectively, where Z_i is the cluster probability and X_i the site probability. Eq. (1) is seen to be correct in the high temperature limit, i.e., $S_m \to S_1$.

The molar equilibrium free energy F_m in the CSA is given by [12]

$$\frac{F_m}{RT} = \gamma \left(\sum_P^{C-1} \sum_{i=1}^n y_P^i \mu_P^i - \ln \lambda \right) - (n\gamma - 1) \sum_P^C \sum_{i=1}^n f_i y_P^i \ln y_P^i, \tag{2}$$

where f_i is the fraction of sublattice of type i, y_P^i is the mole fraction of component P on sublattice i. The μ_P^i are Lagrangian multipliers arising from the mass balance constraints and are related to the species chemical potentials of the atoms on the sublattice i. The cluster partition function, λ, is obtained from the cluster energies and the μ_P^i.

By permitting γ to deviate by a small amount from the value given by $(z/2p)$, it is possible to overcome the problems of the original Yang–Li formulation. Good agreement with the binary alloy fcc prototype phase diagrams derived from either MC simulations or from using the CVM in the tetrahedron approximation can be achieved [12].

3. Results

In order to develop the application of the modified CSA to real multicomponent alloys, we have examined a prototype Cu–Ag–Au fcc order/disorder phase diagram previously calculated by Kikuchi et al. [17] using the CVM. Our object was to use the CVM calculated results as the 'experimental' results. By optimizing the model parameters to these results, slightly different values of pair exchange energies and tetrahedron four-body paramenters were required in the CSA calculations as compared with those used in the CVM calculations. The binary energy parameters used in both the CVM and CSA calculations are listed in Table 1. It should be mentioned that neither calculation involves introducing any ternary interaction parameters nor allowing for any atomic size mismatch and excitational contributions to the free energy. Additionally, in order to obtain asymmetry in the molar energy of mixing, the similar tetrahedron four-body ineractions α_{AB} and α_{BA} are introduced into the CSA calculation

$$\Delta U_m = W_{AB}[3(1 + \alpha_{AB})Z_{AAAB} + 4Z_{AABB} + 3(1 + \alpha_{BA})Z_{ABBB}], \tag{3}$$

where the cluster probabilities Z_{AAAB}, etc., refer to the sum of all combinations of this type. A value of $\gamma = 1.42$ was used in all the calculations. This value having been obtained in the optimization process.

Table 1
Energy parameters used in the calculation of the Cu–Ag–Au ternary phase diagram

	CVM			CSA		
	W (J mol^{-1})	α_{ij}	α_{ji}	W (J mol^{-1})	α_{ij}	α_{ji}
Cu–Au	−5512	0.01	−0.08	−5285	0	−0.08
Cu–Ag	1962	0.2	−0.2	1800	0.2	−0.2
Au–Ag	−4157	0	0	−4000	0	0

W is the pair exchange energy between components and α_{ij}, α_{ji} are tetrahedron four-body parameters with $i,j = 1$, 2 and 3 for component Cu, Au and Ag, respectively.

To compare with the results from the CVM calculation in [17], five isothermal sections were calculated using the CSA at the temperatures of 530, 350, 310, 280 and 240 °C, respectively. It is shown that the results from the CVM and CSA calculation are in very good agreement with each other. Here, we present three of them. The first one was calculated at the higher temperature of 350 °C. The results from using both the CVM and CSA are shown in Figs. 1 and 2, respectively. The CSA phase diagram was calculated using the Pandat software [18]. It can be seen that the isothermal sections from the two calculations are almost identical with one another. A further isothermal section calculated by using the CSA at the temperature of 310 °C is shown in Fig. 4 with the corresponding CVM result being shown in Fig. 3 for comparison. They also are in very good agreement.

The third isothermal section was calculated using the parameters given in Table 1 at the lower temperature of 240 °C. The results from the CVM and CSA calculations are shown in Figs. 5 and 6, respectively. There, it can be seen that the two diagrams are nearly identical but that

an 'island' of the $L1_2$ phase was found to be present in the Au-rich corner from the CSA calculation, although this phase was not reported as being present in the
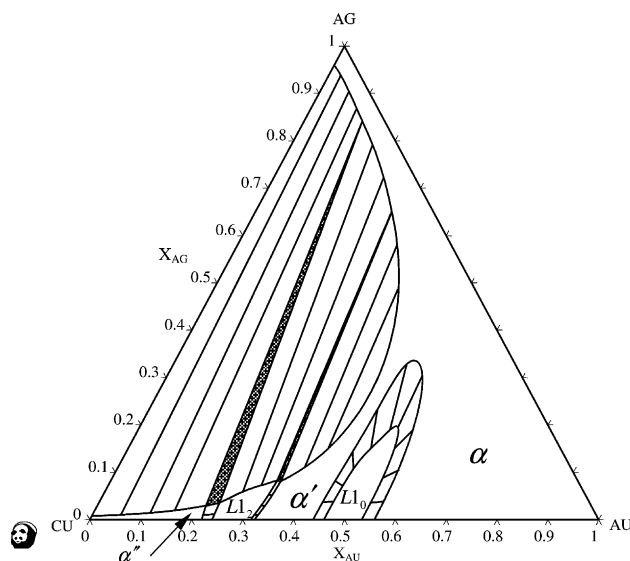

Fig. 2. The prototype Cu–Ag–Au phase diagram calculated by the CSA at 350 °C using the parameters given in Table 1.
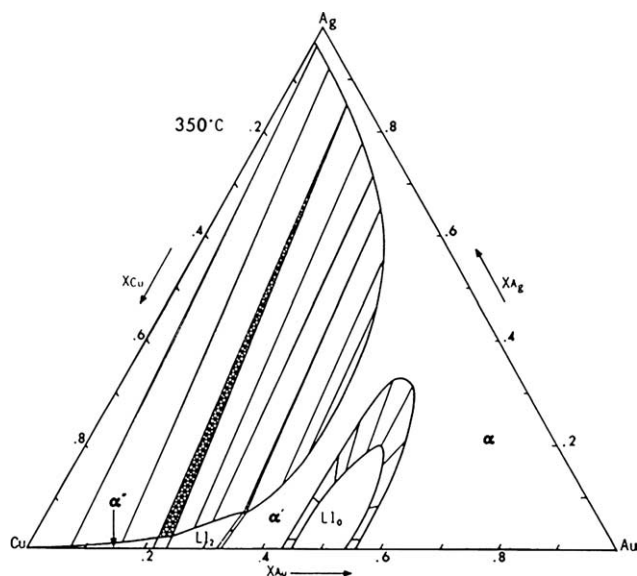

Fig. 1. The prototype Cu–Ag–Au phase diagram calculated by the CVM at 350 °C using the parameters given in Table 1 (from Ref. [17]).
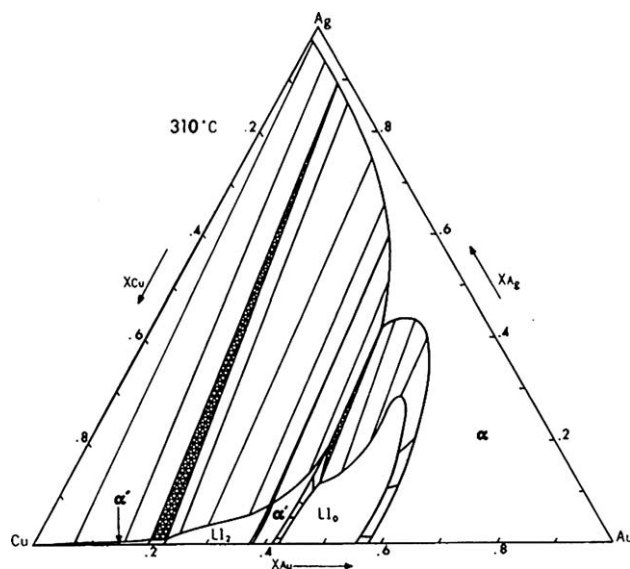

Fig. 3. The prototype Cu–Ag–Au phase diagram calculated by the CVM at 310 °C using the parameters given in Table 1 (from Ref. [17]).
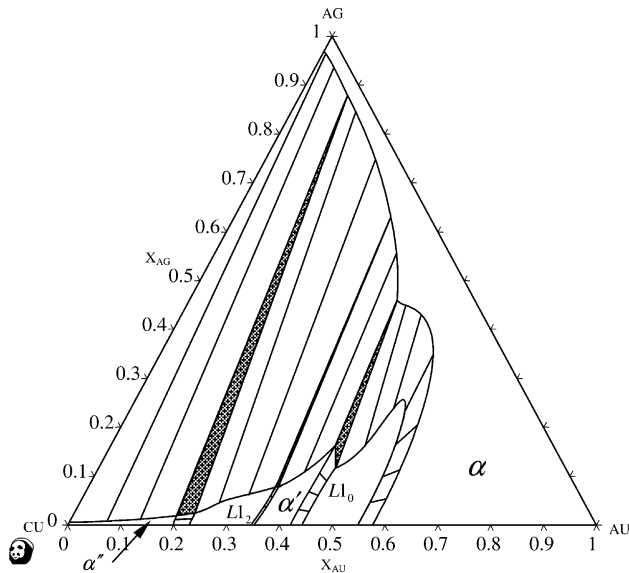
Fig. 4. The prototype Cu–Ag–Au phase diagram calculated by the CSA at 310 °C using the parameters given in Table 1.

Fig. 6. The prototype Cu–Ag–Au phase diagram calculated by the CSA at 240 °C using the parameters given in Table 1.

original CVM calculation. A re-calculation of this part of the CVM diagram [19], reveals that the $L1_2$ 'island' is indeed present there also. In the original CVM calculation, the software used was unable to find the global stable structure unless it was specifically sought and hence why it was overlooked. The Pandat software, on the other hand, is able to obtain the globally lowest Gibbs energy and hence determine the most stable phase state automatically.
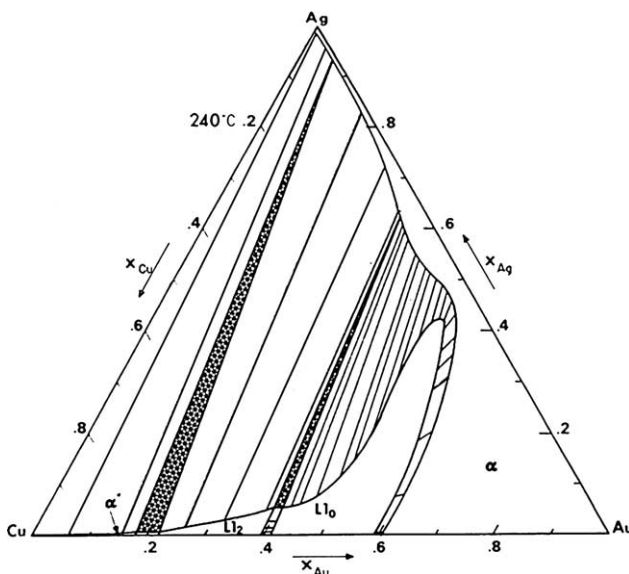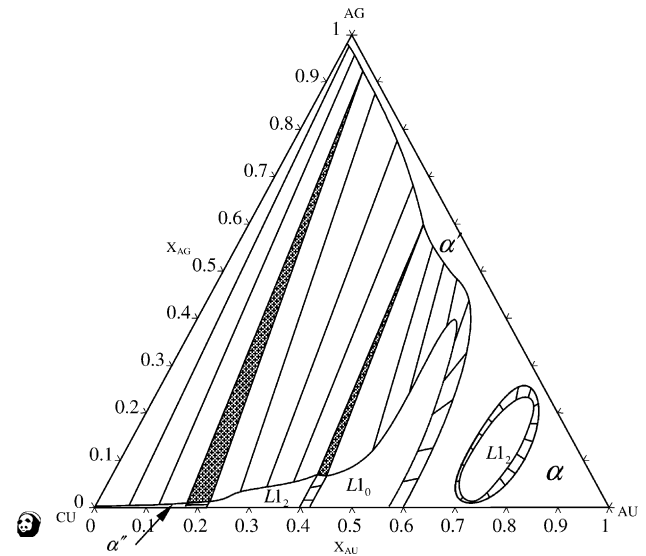
4. Conclusions

Since the clusters in the CSA are, energetically, permitted to share only corners, the corresponding configurational entropy expression includes only two terms and the related free-energy functional is simplified considerably in that the independent variables are the sublattice site occupation probabilities. This is to be contrasted with the CVM where the independent variables are the much more numerous cluster probabilities. It is this reduction in the number of variables which makes the CSA a practical possibility for calculations on multicomponent systems. Despite the considerably reduced computational effort, the present results for some prototype ternary phase diagrams which have been obtained using the CSA are of comparable accuracy to those obtained from using the CVM. This is encouraging for the application of the CSA to real multicomponent alloy systems.

Fig. 5. The prototype Cu–Ag–Au phase diagram calculated by the CVM at 240 °C using the parameters given in Table 1 (from Ref. [17]).

References

[1] Wolverton C, Zunger A. Phys Rev Lett 1995;75:3162.
[2] van de Walle A, Asta M, Ceder G. CALPHAD 2002;26:539.
[3] Saunders N, Miodownik AP. CALPHAD – calculation of phase diagrams, a comprehensive guide. Oxford: Pergamon, Elsevier Science; 1998.
[4] Kikuchi R. Phys Rev 1951;81:988.
[5] Kikuchi R, Van Baal CM. Script Mater 1974;8:425.
[6] Sanchez JM, de Fontaine D. Phys Rev B 1978;17:1926.
[7] Yang CN. J Chem Phys 1945;13:66.
[8] Yang CN, Li Y. Chin J Phys 1947;7:59.
[9] Li Y. J Chem Phys 1949;17:447.
[10] Li Y. Phys Rev 1949;76:972.
[11] Oates WA, Wenzl H. Script Mat 1996;35:623.
[12] Oates WA, Zhang F, Chen S, Chang YA. Phys Rev B 1999;59:11221.
[13] Oates WA. In: Hilpert K, Froben FW, Singheiser L, editors. High Temperature Materials Chemistry, Proceedings of the 10th International IUPAC Conference, Jülich, Germany, April 2000, vol. 15. Germany: Forschungszentrum Jülich GmbH, Jülich; 2000. p. 229–34.
[14] Zhang J et al. Intermetallics 2001;9:5.
[15] Zhang F, Chen S-L, Chang YA, Oates WA. Intermetallics 2001;9:1079.
[16] Zhang F et al. Acta Mater 2003;51:207.
[17] Kikuchi R, Sanchez JM, deFontaine D, Yamauchi H. Acta Metall 1980;28:651.
[18] PANDAT™ Software for Multicomponent Phase Diagram Calculation is available from Computherm LLC, 437 S. Yellowstone Drive, Suite 217, Madison, WI 53719, USA.
[19] CVM calculation carried out by Prof. C. Colinet.